

Supporting information

Role of Anatase/TiO₂(B) heterointerface for ultrastable high-rate lithium and sodium energy storage performance

Guilong Liu^a, Hong-Hui Wu^{*b, c}, Qiangqiang Meng^d, Ting Zhang^a, Dong Sun^a,
Xueyang Jin^a, Donglei Guo^a, Naiteng Wu^a, Xianming Liu^{*a}, Jang-Kyo Kim^{*c}

^a Key Laboratory of Function-oriented Porous Materials of Henan Province, College of Chemistry and Chemical Engineering, Luoyang Normal University, Luoyang 471934, Henan, P. R. China.

^b Beijing advanced innovation center for materials genome engineering, State Key Laboratory for Advanced Metals and Materials, University of Science and Technology Beijing, Beijing 100083, China

^c Department of Mechanical and Aerospace Engineering, Hong Kong University of Science and Technology, Clear Water Bay, Kowloon, Hong Kong, P. R. China.

^d Key Laboratory for Advanced Technology in Environmental Protection of Jiangsu Province, Yancheng Institute of Technology, Yancheng, P. R. China

*Corresponding author: *Tel*: +86 0379 68618325

Email address: myclxm@163.com (Xianming Liu); hhwuuaa@connect.ust.hk (Hong-Hui Wu); mejkkim@ust.hk (Jang-Kyo Kim).

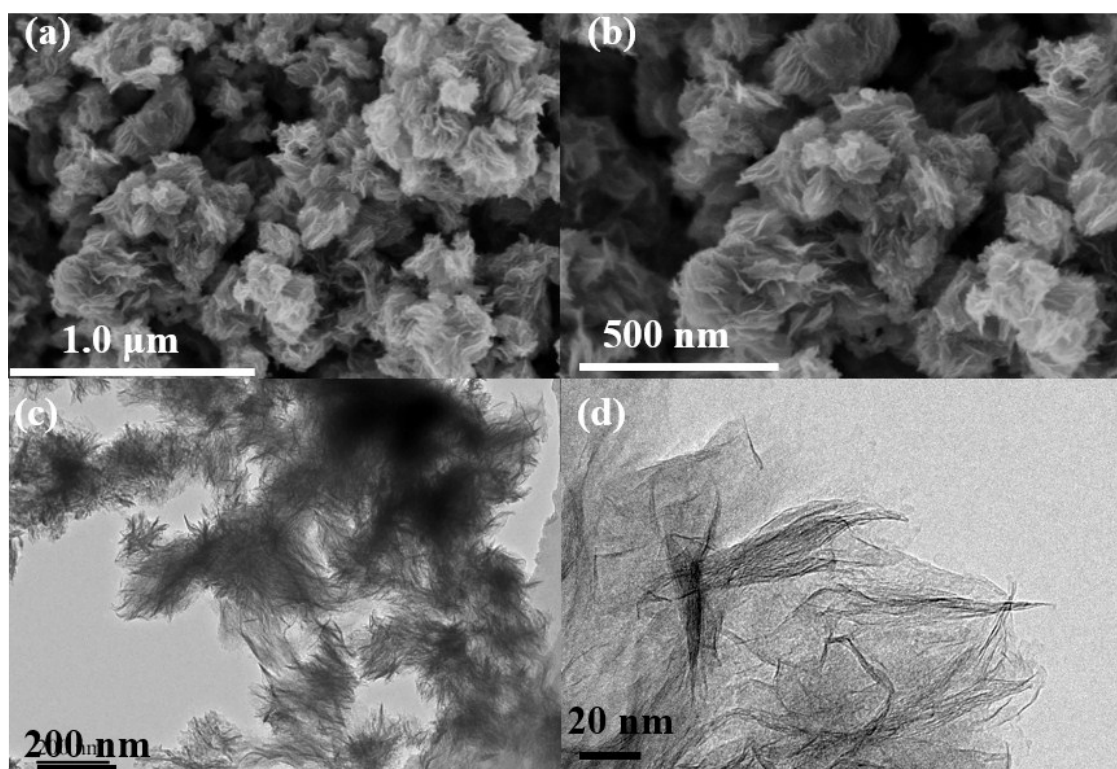


Fig. S1 (a, b) SEM and (c, d) TEM images of TAB/C precursor.

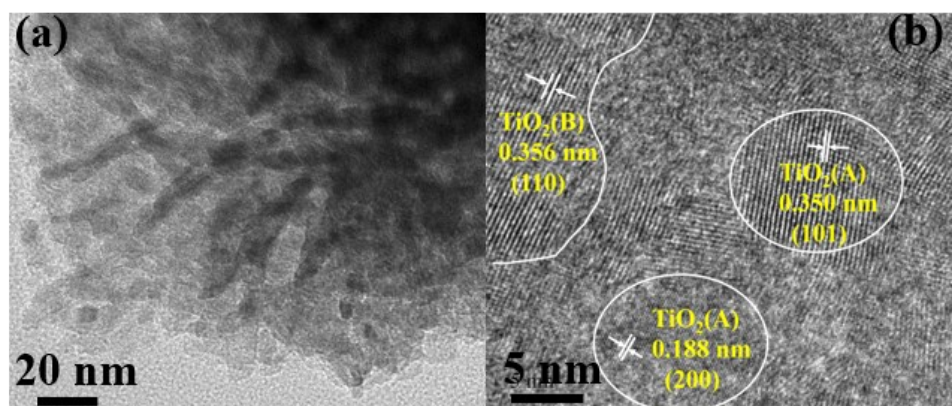


Fig. S2 HRTEM images of TAB.

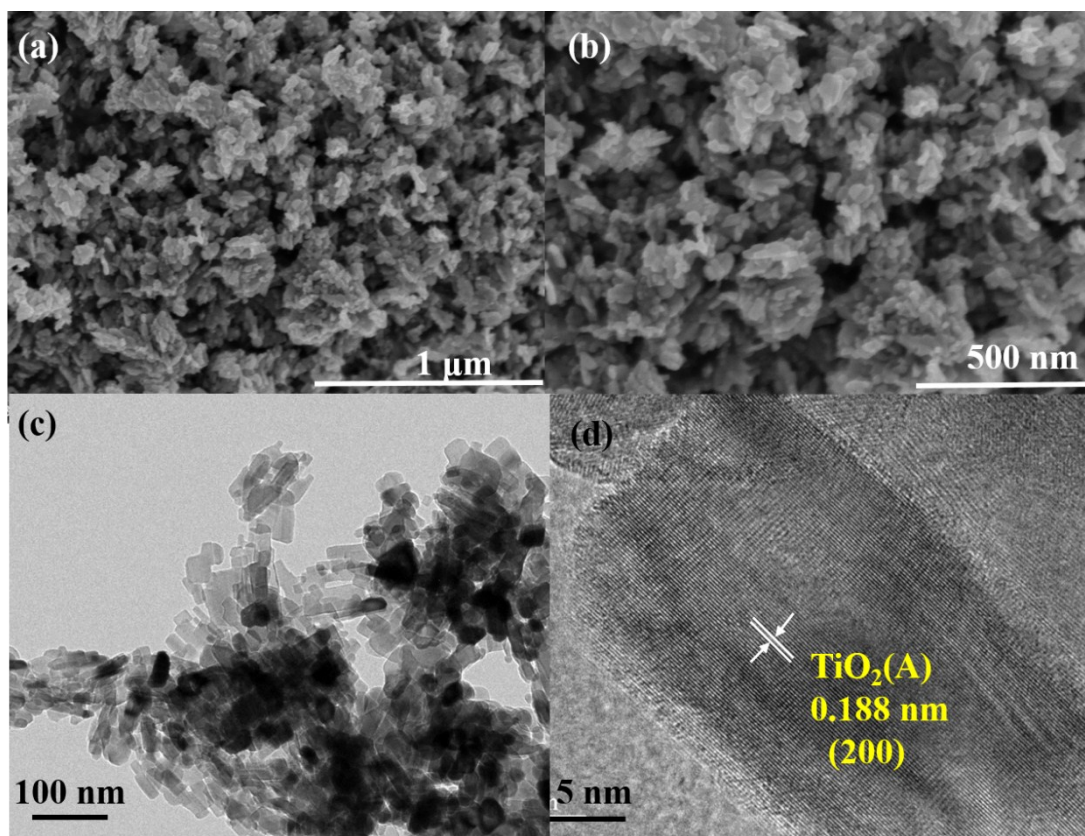


Fig. S3 (a, b) SEM and (c, d) TEM images of TA nanoparticles.

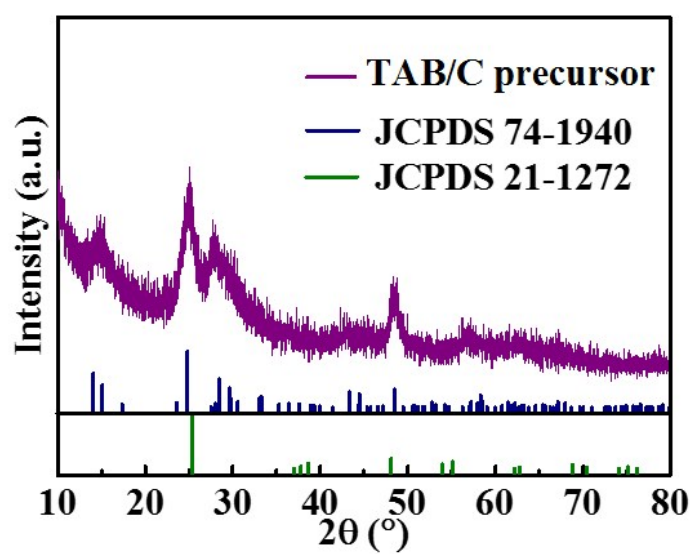


Fig. S4 XRD pattern of TAB/C precursor.

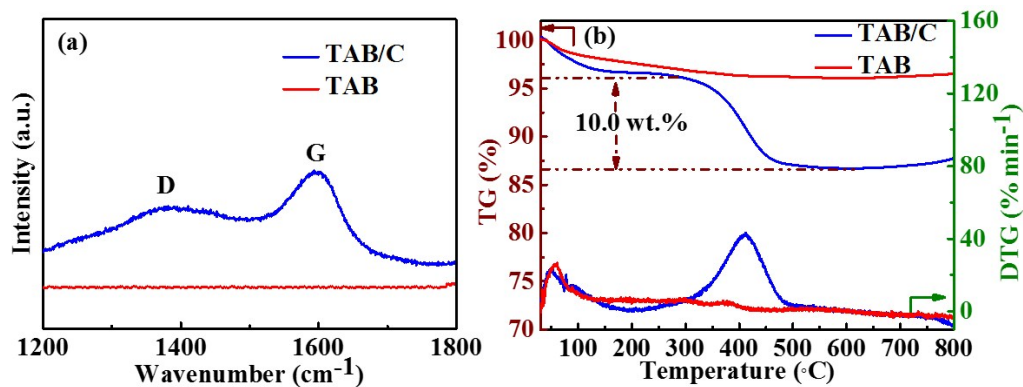


Fig. S5 (a) Raman spectra and (b) TGA curves of TAB/C and TAB.

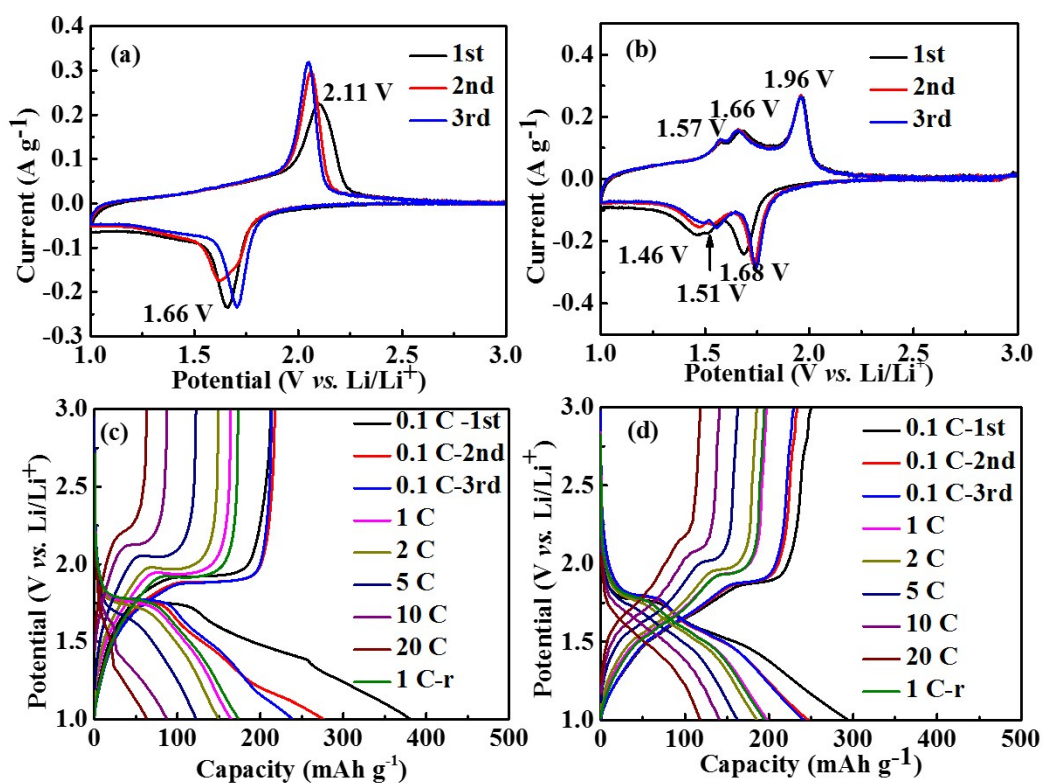


Fig. S6 CV curves at 0.1 mV s^{-1} of (a) TAB and (b) TAB/C for LIBs; galvanostatic charge/discharge (GCD) curves of (c) TAB and (d) TAB/C for LIBs, where the label 1 C-r represents the result when the current density reverts from 20 C to 1 C.

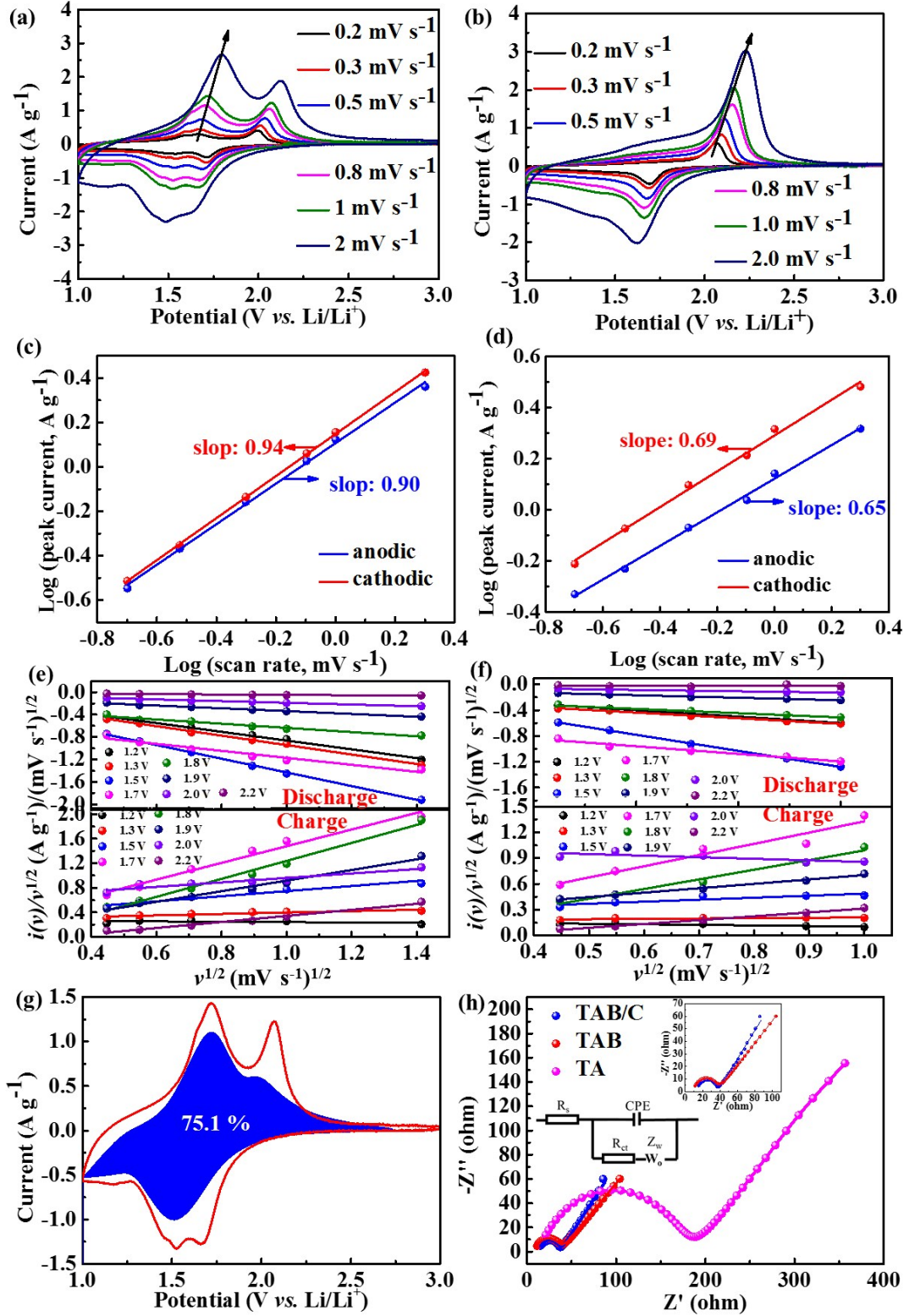


Fig. S7 Kinetics analysis for LIBs: CV curves at different scan rates of (a) TAB and (b) TA; log(*i*)-log(*v*) plots of CV curves to determine *b*-values of (c) TAB and (d) TA; $i(v)/v^{1/2}$ vs. $v^{1/2}$ at different potentials during charge/discharge cycles of (e) TAB/C and (f) TAB; (g) capacitive contribution (blue region) of TAB at 0.8 mV s⁻¹; (h) EIS

spectra of the TAB/C, TAB and TA electrodes after 1000 cycles at 10 C, inserts are the equivalent circuit model and the enlarged view of EIS.

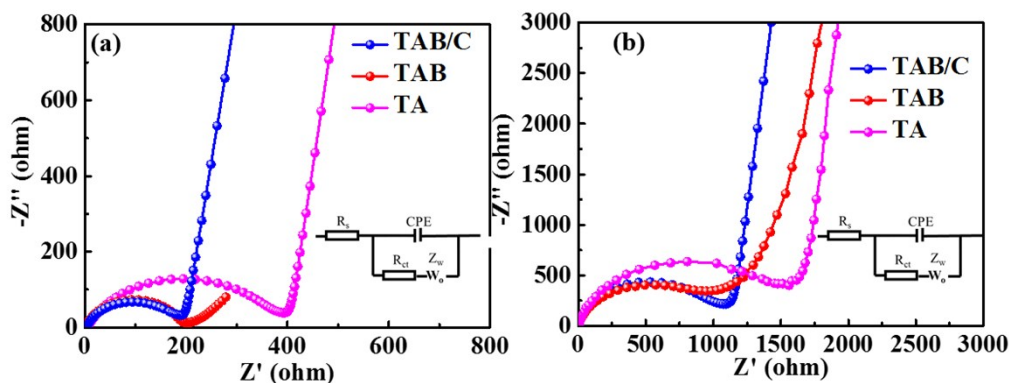


Fig. S8 EIS spectra of the TAB/C, TAB and TA electrodes in (a) LIBs and (b) SIBs before cycles, inserts are the equivalent circuit models.

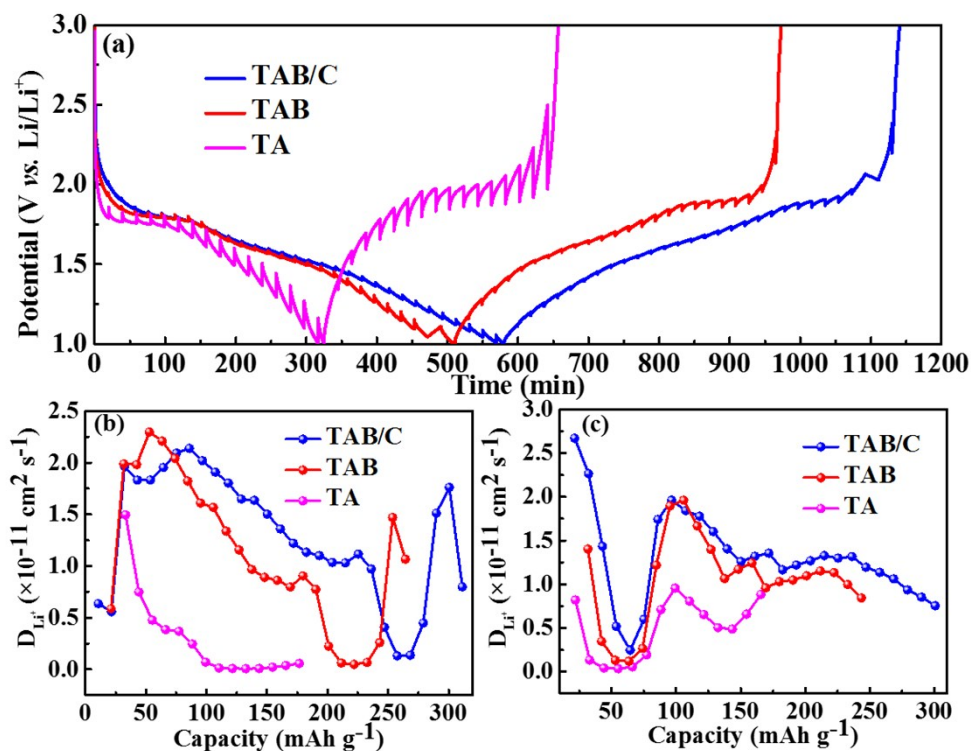


Fig. S9 (a) GITT profiles for LIBs; D_{Li^+} as a function of (b) discharge capacity and (c) charge capacity for LIBs.

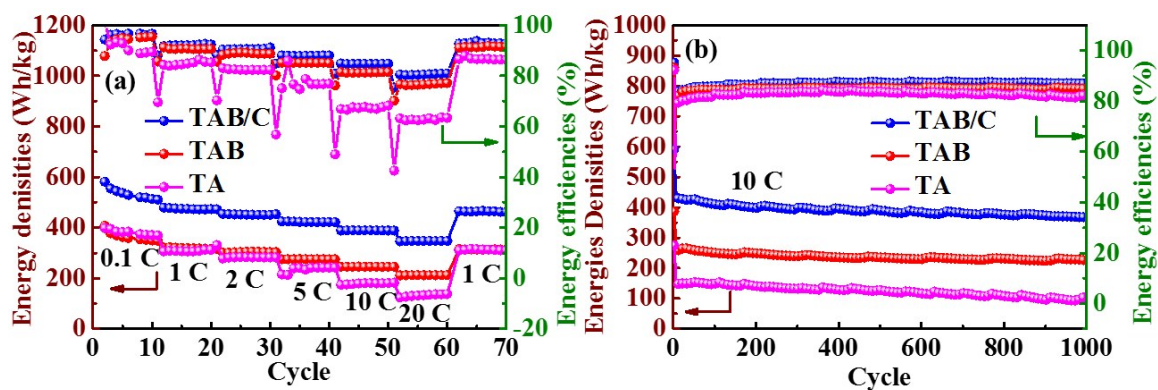


Fig. S10 Energy densities and energy efficiencies of the TAB/C, TAB and TA electrodes for LIBs during rate (a) and cycle (b) tests.

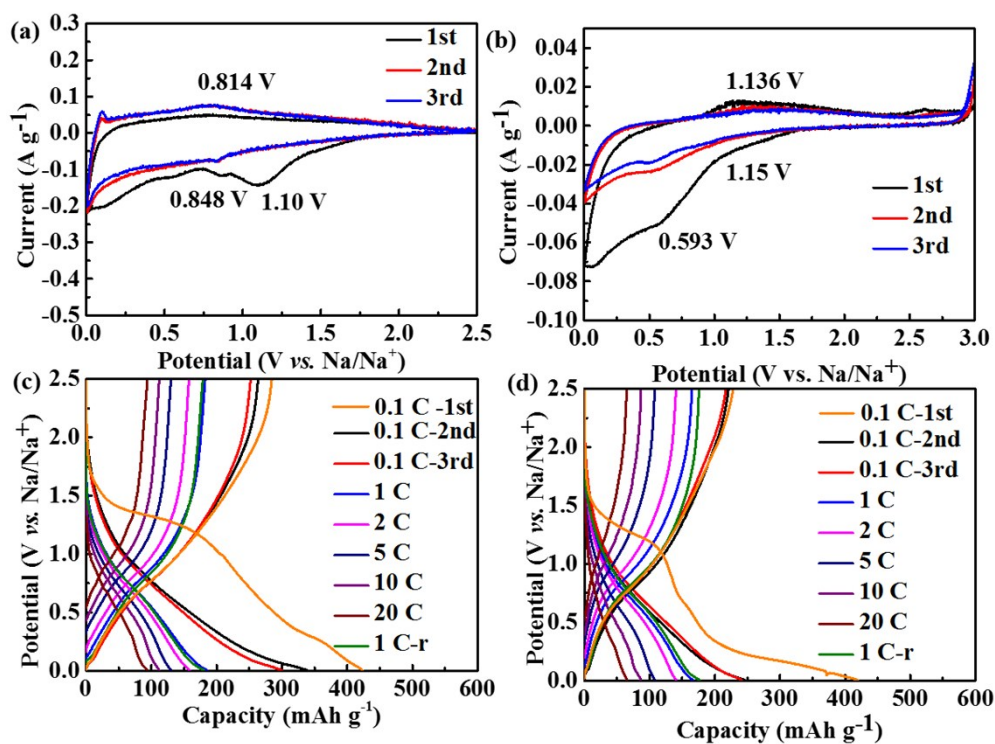


Fig. S11 CV curves at 0.1 mV s⁻¹ of (a) TAB and (b) TA for SIBs; GCD curves of (c) TAB and (d) TA for SIBs, where the label 1 C-r represents the result when the current density reverts from 20C to 1 C.

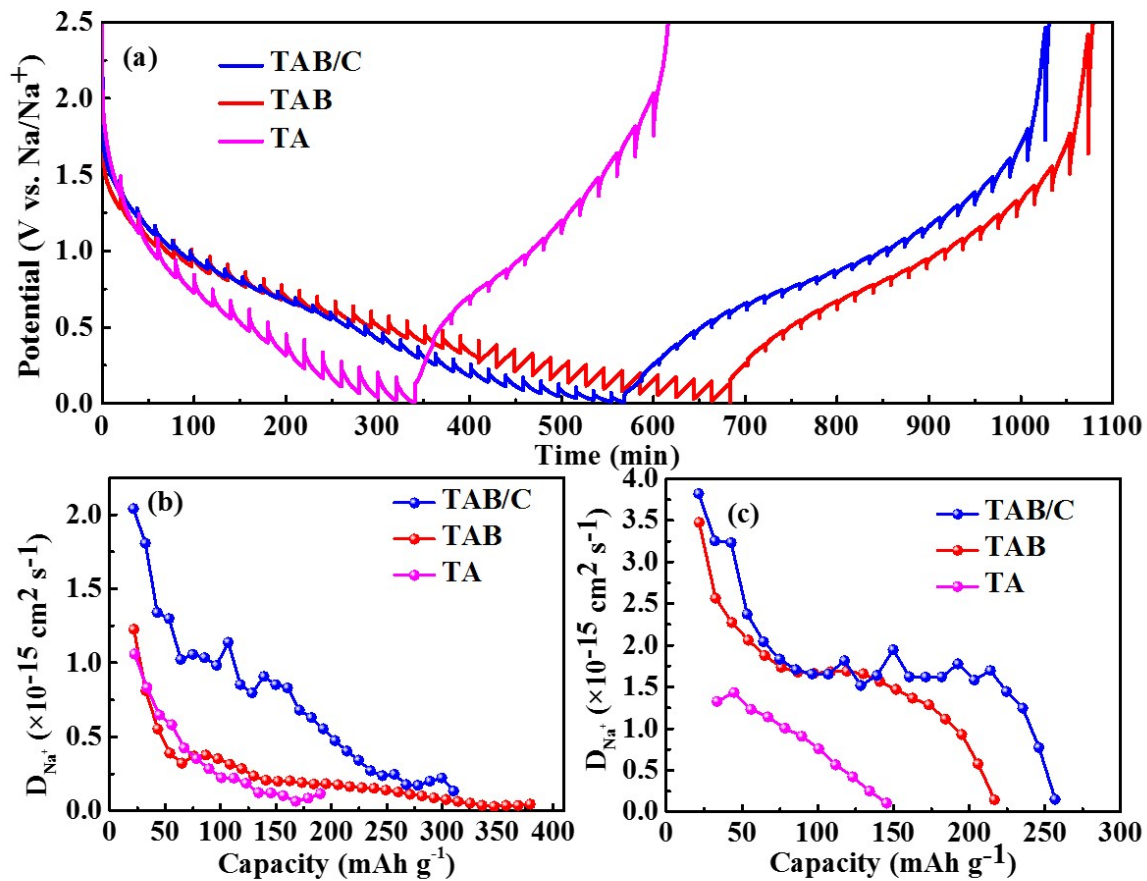


Fig. S12 (a) GITT profiles for SIBs; D_{Na^+} as a function of (b) discharge capacity and (c) charge capacity for SIBs.

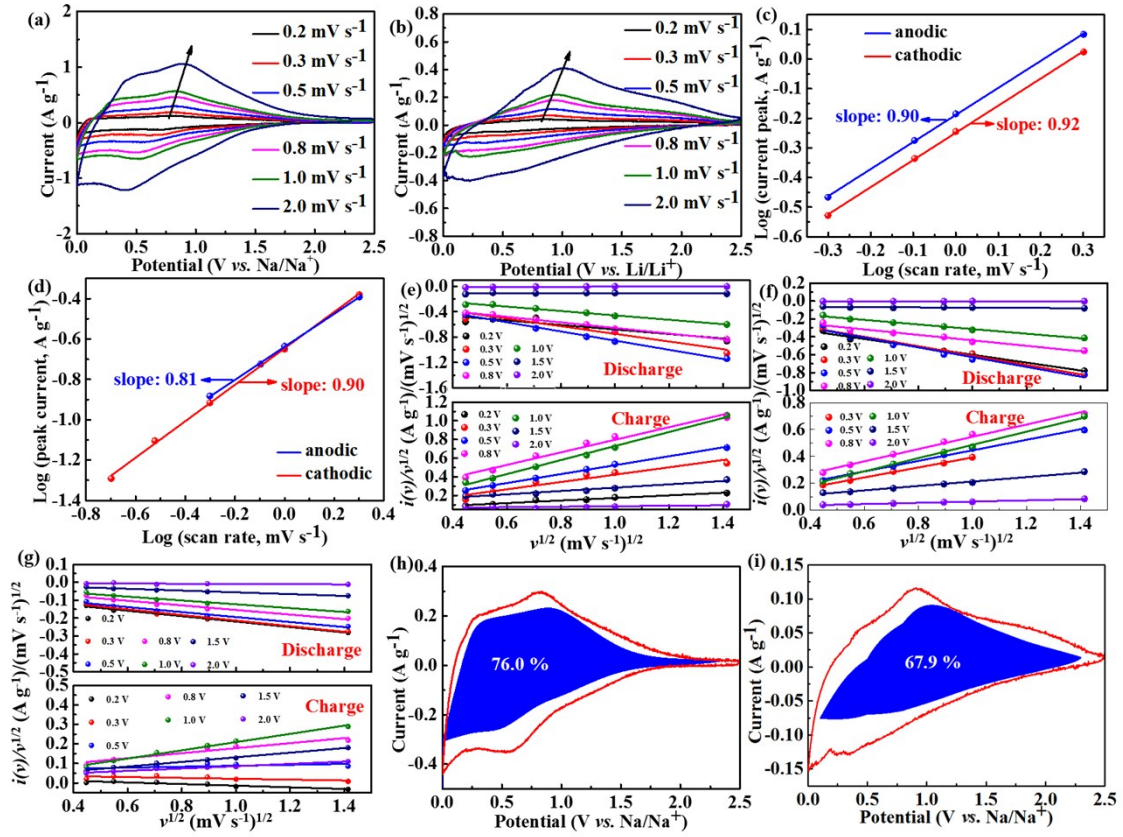


Fig. S13 Kinetics analysis of SIBs: CV curves at different scan rates of (a) TAB and (b) TA; $\log(i)$ - $\log(v)$ plots of CV curves to determine b -values of (c) TAB and (d) TA; $i(v)/v^{1/2}$ vs. $v^{1/2}$ at different potentials during charge/discharge cycles for (e) TAB/C, (f) TAB and (g) TA; capacitive contributions (blue region) of (h) TAB and (i) TA at 0.5 mV s^{-1} .

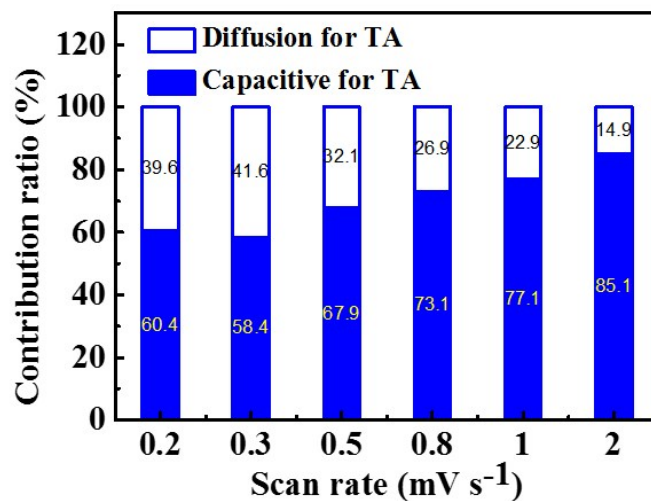


Fig. S14 Capacity contributions from diffusion-controlled and capacitive behaviors of the TA electrode at different scan rates for SIBs.

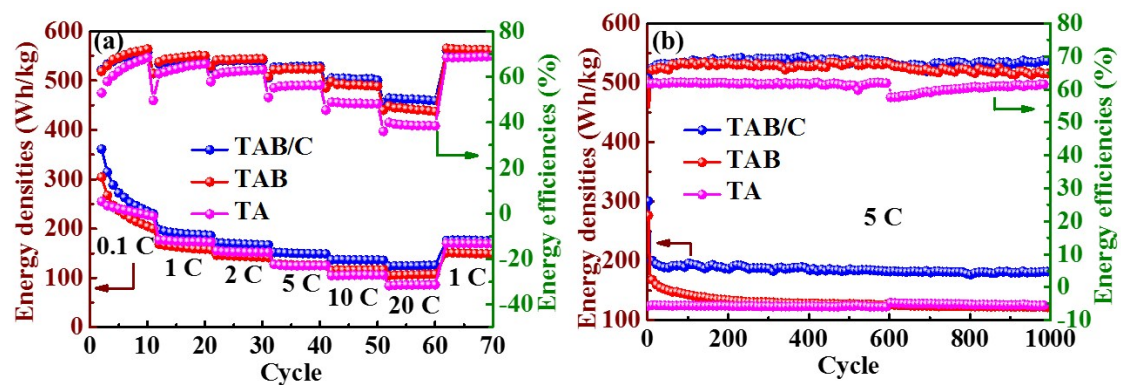


Fig. S15 Energy densities and energy efficiencies of the TAB/C, TAB and TA electrodes for SIBs during rate (a) and cycle (b) tests.

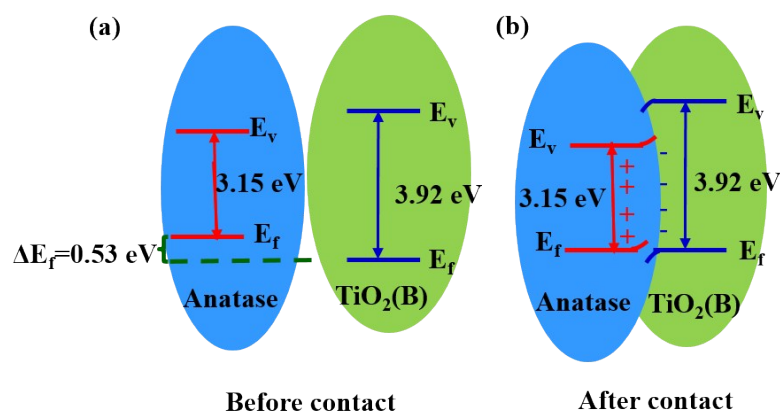


Fig. S16 Formation mechanism and direction of the internal electric field when the heterostructure is formed from the anatase and $\text{TiO}_2(\text{B})$ phases: (a) before and (b) after formation.

Table S1 Surface area and pore volume of TAB/C and TAB.

Electrode materials	Surface area ($\text{m}^2 \text{g}^{-1}$)	Pore volume ($\text{cm}^3 \text{g}^{-1}$)
TAB/C	125	0.55
TAB	95	0.45

Table S2 Impedance parameters of the TAB/C, TAB and TA electrodes before and after 1000 cycles for LIBs and SIBs.

Battery systems	Electrode materials	Fresh electrodes		Electrodes after cycles	
		R_s/Ω	R_{ct}/Ω	R_s/Ω	R_{ct}/Ω
LIBs	TAB/C	4.1	170.4	12.9	24.2
	TAB	2.2	182.9	9.0	28.5
	TA	5.5	368.6	8.5	111.8
SIBs	TAB/C	4.0	785.1	6.6	129.9
	TAB	3.9	955.0	3.3	308.5
	TA	4.5	1372.0	13.2	334.5

Table S3 Electrochemical performance of state-of-the-art TiO₂-based anode materials for LIBs and SIBs.

Materials	Battery system	Cyclic performance ^a	Rate performance ^a	Reference
TAB/C	LIBs	212 mAh g⁻¹ after 1000 cycles at 10 C	193 mAh g⁻¹ at 20 C	This work
AB550		190 mAh g ⁻¹ after 1000 cycles at 10 C	150 mAh g ⁻¹ at 20 C	41
TiO ₂ (AB)-2		103 mAh g ⁻¹ after 1000 cycles at 10 C	80 mAh g ⁻¹ at 20 C	6
TAB Nanowires		-	160 mAh g ⁻¹ at 20 C	58
TAB300		210 mAh g ⁻¹ after 60 cycles at 2 C	110 mAh g ⁻¹ at 20 C	40
TiO ₂ (B)-HTs		160 mAh g ⁻¹ after 400 cycles at 10 C	160 mAh g ⁻¹ at 20 C	35
TiO _{2-x} /CNT		~160 mAh g ⁻¹ after 1000 cycles at 6 C	155 mAh g ⁻¹ at 12 C	33
TiO ₂ /RGO		130 mAh g ⁻¹ after 1000 cycles at 10 C	152 mAh g ⁻¹ at 10 C	12
H-TiO ₂ @C ^b		126 mAh g ⁻¹ after 200 cycles at 6 C	50 mAh g ⁻¹ at 10 C	29
TiO _{2-x} /GQDs		168 mAh g ⁻¹ after 100 cycles at 10 C	155 mAh g ⁻¹ at 20 C	27
Hollow TiO ₂		195 mAh g ⁻¹ after 600 cycles at 0.6 C	196 mAh g ⁻¹ at 6 C	25
TAB/C		173 mAh g⁻¹ after 1000 cycles at 5 C	112 mAh g⁻¹ at 20 C 144 mAh g⁻¹ at 10 C	This work
TAB300 ^b		80 mAh g ⁻¹ after 30 cycles at 0.2 C	-	40
TiO ₂ (B) belts ^b		211 mAh g ⁻¹ after 500 cycles at 1 C	106 mAh g ⁻¹ at 20 C	38

TiO ₂ (B) wires		150 mAh g ⁻¹ after 50 cycles at 0.12 C	82.3 mAh g ⁻¹ at 1.2 C	S1
TiO _{2-x} /CNT	SIBs	~140 mAh g ⁻¹ after 1000 cycles at 6 C	118 mAh g ⁻¹ at 12 C	33
TiO ₂ nanotubes		126 mAh g ⁻¹ after 100 cycles at 1 C	129 mAh g ⁻¹ at 10 C	52
C coupled TiO ₂		100 mAh g ⁻¹ after 2000 cycles at 20 C	111 mAh g ⁻¹ at 20 C	20
TiO ₂ /NC ^b		137 mAh g ⁻¹ after 1000 cycles at 10 C	104 mAh g ⁻¹ at 20 C	23
TiO ₂ @CNTs/CFP ^b		179 mAh g ⁻¹ after 400 cycles at 12 C	129 mAh g ⁻¹ at 12 C	24
TiO ₂ @NFG		146 mAh g ⁻¹ after 8000 cycles at 10 C	129 mAh g ⁻¹ at 20 C	3

^a 1 C=168 mAh g⁻¹.

^b Data obtained in the potential range of 0.05 – 3.0 V.

References

S1. J. Lee, J. K. Lee, K. Y. Chung, H. G. Jung, H. Kim, J. Mun and W. Choi,. *Electrochim. Acta* 2016, **200**, 21-28.